

## Spectral and magnetic interplay in quantum spin chains: Stabilization of the critical phase due to long-range order

Indubala I. Satija\*

*Department of Physics and Institute of Computational Sciences and Informatics, George Mason University, Fairfax, VA 22030*  
(Received 27 July 1993; revised manuscript received 19 October 1993)

The anisotropic quantum  $XY$  spin chain in a modulating magnetic field incommensurate with the periodicity of the chain is studied. Using Jordan-Wigner transformation, the model is mapped to a tight-binding model in fermions. In the absence of symmetry-breaking terms, the fermion model is identical with the well-known Harper equation exhibiting extended and localized phases with the onset of transition being a critical point with fractal spectrum and wave functions. The effect of  $O(2)$  symmetry breaking is to fatten the critical point resulting in a critical phase with power-law localization existing in a finite window of size determined by the anisotropy. In this three-phase spectral diagram, the transition from critical to localized phase is accompanied by the magnetic transition to long-range order. Furthermore, the scaling properties of the fractal spectrum vary in the critical phase. This leads to interesting consequences on the low-temperature thermodynamical properties of the system.

### I. INTRODUCTION

The one dimensional Harper equation,<sup>1</sup>

$$\psi_{i+1} + \psi_{i-1} + \lambda \cos(2\pi\sigma n)\psi_n = E\psi_n, \quad (1)$$

is considered a paradigm in the study of quasiperiodic (QP) systems exhibiting metallic or Bloch-type extended ( $E$ ) states and insulating or exponentially localized ( $L$ ) states for irrational  $\sigma$ .<sup>2</sup> At the onset of a metal-insulator transition, the states are critical ( $C$ ) with power-law localization characterized by fractal spectrum and wave functions. The exotic self-similar energy spectrum, known as the butterfly spectrum,<sup>3</sup> has triggered a great deal of interest in this model. Furthermore since QP systems are in between periodic and random systems (having localized states in one dimension), they provide a useful link for understanding the crossover between periodic and random systems. The Harper model has also been extensively studied in other contexts such as two-dimensional periodic crystals in a magnetic field. Here the problem of a two-dimensional electron gas in the presence of a field is reduced to the one-dimensional Harper equation.<sup>2</sup> The model has also generated a great deal of interest due to its connection to the quantized Hall effect<sup>4</sup> and mean-field theory of the Hubbard model.<sup>5</sup> Very recently, attempts have been made to obtain an experimental realization of the exotic  $C$  phase in two-dimensional mesoscopic systems and in fact some signatures of the self-similar butterfly spectrum have been experimentally observed.<sup>6</sup> The Harper equation is also of great interest in the theory of nonintegrable Hamiltonian systems due to its correspondence with the two-dimensional area preserving maps. The weak coupling limit of the two problems shares a common mathematical problem with the small divisor perturbation theory of KAM.<sup>7</sup> The smooth Bloch states of the Harper model are analogous to the KAM tori of the area preserving maps while the discon-

tinuous  $L$  states bear a close resemblance to the Cantori. This clear-cut correspondence between the eigenstates of the Harper map and the invariant point sets of two-dimensional area preserving maps<sup>8</sup> leads to a common paradigm for breakdown of analyticity in nonlinear low-dimensional QP systems.

In this paper, our interest in the Harper equation originated from the fact that the Harper equation describes the isotropic  $XY$  quantum spin-1/2 chain in a sinusoidally varying transverse magnetic field of periodicity incommensurate with the period of the chain. The Jordan-Wigner transformation reduces the spin problem to a tight-binding model (TBM) for the fermions. Specifically, we address the question of how the metal-insulator transition and the critical point of Harper are affected by the breaking of the  $O(2)$  symmetry of the  $XY$  model. The anisotropic model has long-range magnetic correlations in the  $XY$  spin space. The presence of transverse magnetic field introduces a competition between the spin alignment in and out of the  $XY$  plane resulting in a magnetic transition to long-range order (LRO). We investigate the correlations between the spectral and magnetic transitions in the model.

Our studies show that in the presence of anisotropy, the  $C$  phase is a fat set (of finite measure) in parameter space sandwiched between the  $E$  and  $L$  phases. Stated differently, the anisotropy fattens or stabilizes the critical point of the Harper model. Both the  $E$  and  $C$  phases sustain finite long-range magnetic correlations in the  $XY$  spin plane while in the localized phase the in-plane magnetic correlations vanish. Therefore, the transition to localization is accompanied by the transition from a magnetically ordered to a disordered phase. Unlike the periodic case, where the onset of LRO is determined by the sum of exchange interactions along the easy and hard axes, in the QP case this onset is solely determined by the strength of exchange interaction along the easy axes.

A short description of these results was presented in an earlier paper.<sup>9</sup>

In Sec. I, we obtain the fermion representation of the quantum spin chains and review some of the properties of the periodic spin chain and the Harper equation. In Secs. II and III, we, respectively, study the spectral and magnetic properties of the model. In Sec. IV, we study the global scaling properties of the cantor spectrum. In Sec. V, we investigate the effects of higher harmonics and show that unlike the isotropic model, the anisotropic model does not exhibit fractal boundary between the  $E$  and  $L$  phases. In Sec. VI, we summarize our results.

## II. ANISOTROPIC SPIN CHAIN IN A TRANSVERSE FIELD

We study the anisotropic  $XY$  model in a QP magnetic field.

$$H = - \sum_n [J_x \sigma_n^x \sigma_{n+1}^x + J_y \sigma_n^y \sigma_{n+1}^y + h_n \sigma_n^z]. \quad (2)$$

The magnetic field is chosen to be a sinusoidal function with a period incommensurate with the periodicity of the lattice,

$$h_n = \lambda \cos(2\pi\sigma n), \quad (3)$$

where  $\sigma$  is an irrational number, which, for convenience, we will choose to be the golden mean,  $\sigma = [\sqrt{5} - 1]/2$ , however, results of this paper do not depend upon this choice. The parameter  $\lambda$  is the strength of the QP field. The spin space anisotropy  $g$  is given by

$$g = J_y - J_x. \quad (4)$$

For  $g = 0$ , the isotropic model is the  $XY$  model while  $g = -1$ , the model reduces to the Ising model. For any finite value of  $g$ , the model is Ising-like due to  $O(1)$  symmetry and hence at zero temperature, and in the absence of any magnetic field, spins will align along an axis in the  $XY$  plane. This axis of spin alignment in the plane will be referred to as the easy axis while the axis perpendicular to the easy axis in the plane is called the hard axis. Clearly, for  $J_x > J_y$ , the  $x$  axis will be the easy axis and for  $J_x < J_y$ , the  $y$  axis will be the easy axis. As we will see later, it is convenient to label the exchange interactions along the easy and hard axes by  $J_e$  and  $J_h$ , respectively.

Using Jordan-Wigner transformation, the spin models are mapped to fermion models, quadratic in fermion degrees of freedom:<sup>10</sup>

$$H = - \sum [c_n^\dagger A_{nm} c_m + c_n^\dagger B_{nm} c_m^\dagger + \text{H.c.}]. \quad (5)$$

Here,  $c_n$  are the anticommuting fermion operators. The matrices  $A$  and  $B$  are, respectively, the symmetric and antisymmetric matrices with nonzero elements defined as  $A_{n,n} = 2h_n$ ,  $A_{n,n+1} = J_x + J_y$ ,  $B_{n,n+1} = J_x - J_y = -g$ . Therefore, the presence of the fermion nonconserving term is due to the existence of anisotropy. It is this term which results in long-range correlations among spins. Us-

ing the method described by Lieb *et al.*<sup>10</sup> the diagonalization of the above quadratic form reduces to diagonalizing the matrix  $(A+B)(A-B)$ . The resulting eigenvalue equation can be written as a TBM:

$$\begin{aligned} E^2/4\psi_n = & J_x J_y (\psi_{n-2} + \psi_{n+2}) \\ & + (J_y h_{n-1} + J_x h_n) \psi_{n-1} \\ & + (J_y h_n + J_x h_{n+1}) \psi_{n+1} \\ & + (J_x^2 + J_y^2 + h_n^2) \psi_n. \end{aligned} \quad (6)$$

It is interesting to note that in the pure  $XY$  limit ( $J_x = J_y = J$ ), the above TBM is identical to the Harper equation squared. Both the Ising and  $XY$  limits are special cases where the TBM underlying the spin system involves only a nearest-neighbor (NN) interaction among fermions. Therefore, the existence of a next-nearest-neighbor (NNN) interaction seems to be related to the existence of two distinct axes in spin space.<sup>11</sup>

The periodic model ( $\sigma = 1$ ) can be solved analytically in the sense that the wave functions and energies can be determined. The fermion states are always extended and the energy spectrum has a gap (for nonzero anisotropy) which vanishes at a critical value of  $\lambda = J_x + J_y$  corresponding to the flipping of the spins from the plane to the  $z$  axis resulting in the vanishing of magnetic long-range correlations in the  $XY$  plane. In the Ising limit, duality transformation (between the site and bond variables) can also be exploited<sup>12</sup> to infer the magnetic transition to LRO.

The Harper equation or  $O(2)$  spin chain in a QP transverse field has a dual representation in the Fourier space and has been shown to be self-dual<sup>13</sup> at  $\lambda = 2J$ . The self-dual point is the onset of an  $E$ - $L$  transition exhibiting fractal spectrum. The presence of anisotropy breaks the  $O(2)$  symmetry and destroys the self-duality. Therefore, self-duality of the Harper equation can be viewed from a different perspective: it is due to the  $O(2)$  symmetry of the  $XY$  model when the easy and hard axes of the model degenerate.

## III. SPECTRAL PHASE DIAGRAM

Ground state properties of the QP anisotropic spin chain were studied by numerical diagonalization of the TBM [Eq. (6)]. This requires diagonalizing the TBM for various chain sizes or Fibonacci orders  $F_l$  ( $\sigma = F_{l-1}/F_l$ ) corresponding to various rational approximants of the golden mean. We then use finite size scaling arguments to distinguish between the  $E$ ,  $C$ , and  $L$  phases. In our systematic study, for different values of  $g$  and  $\lambda$ , the energy spectrum and wave functions were calculated. Under periodic boundary conditions  $\psi_{n+F_l} = e^{ikF_l} \psi_n$  where  $k$  is the Bloch index, the energy spectrum of the TBM consists of  $F_l$  bands separated by  $F_l - 1$  gaps.

In analogy with the self-dual isotropic model, the anisotropic models for all values of  $g$  were found to exhibit a pure spectrum: i.e., all the quantum states were either extended, critical, or localized simultaneously. Unlike the isotropic case, the  $E$  phase is always massive signaling the broken symmetry resulting in long-range

correlations among the spins (see Sec. IV). To infer the spectral phase diagram for fixed  $g$  as a function of  $\lambda$ , we compute the total bandwidth (TBW) of the energy spectrum, the participation ratio  $P = 1/\sum |\psi_n|^4$ . Here,  $\psi_n$  are the normalized wave functions of the fermions on the lattice. The finite size scaling arguments as described below are then used to label various phases. The TBW of the chain of  $F_l$  spins is found to vary as  $F_l^{-\delta}$ . The exponent  $\delta$  is, respectively, 0 and  $\infty$  in the  $E$  and  $L$  phases and is finite in the  $C$  phase. Hence in the  $E$  phase TBW is independent of the size of the chain and in the  $L$  and  $C$  phases it, respectively, exhibits exponential and power-law decay with the size of the spin chain. In the  $C$  phase, for all values of  $g$  and  $\lambda$ , the exponent  $\delta$  was found to be close to unity. The participation ratio  $P$  was also found

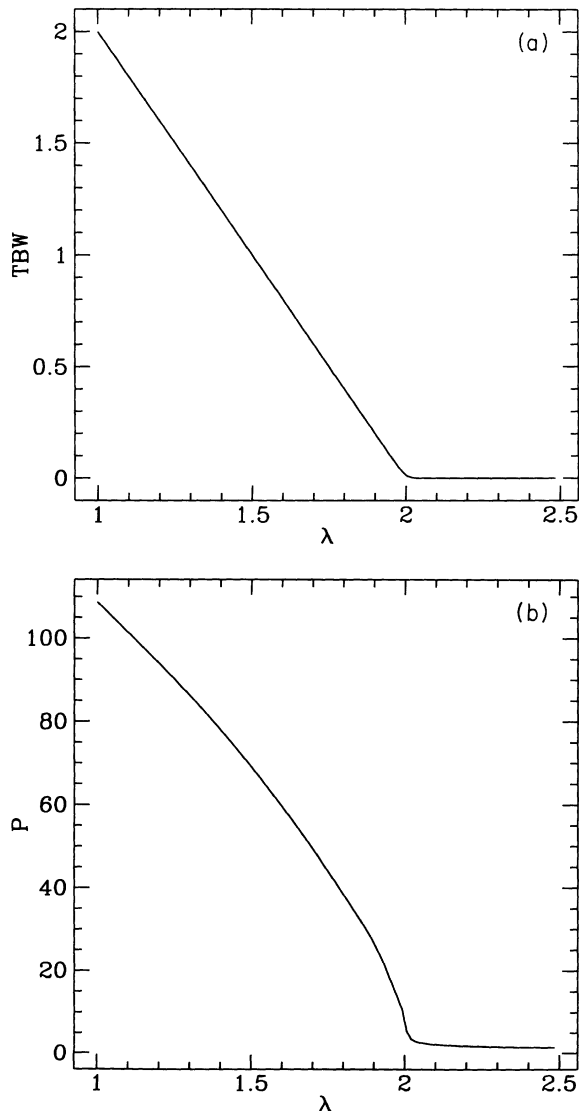


FIG. 1. (a)-(b) show the TBW and  $P$  for the isotropic model ( $g = 0$ ) ( $\sigma = 233/377$ )  $J = 1$ . Beyond  $\lambda = 2$ , the states are exponentially localized and  $P$  is of the order of unity.

to clearly distinguish the  $E$ ,  $L$ , and  $C$  phases:  $P$  was of the order of size of the system in the  $E$  phase and of the order of unity in the  $L$  phase, whereas in the  $C$  phase, it was in between these two limiting cases.

Comparing Figs. 1 and 2, we see that the single  $E$ - $L$  transition of the isotropic model in the presence of anisotropy, is split into two transitions: namely,  $E$ - $C$  and  $C$ - $L$ . Therefore, the anisotropy fattens the critical point to a fat set resulting in the three-phase diagram where each of the  $E$ ,  $C$ , and  $L$  phases exist in a finite window in the parameter  $\lambda$ . Our numerical results show that the onset of  $E$ - $C$  transition is at  $\lambda = 2J_h$  while that of the  $C$ - $L$  transition is at  $\lambda = 2J_e$ . Therefore the onsets of  $E$ -

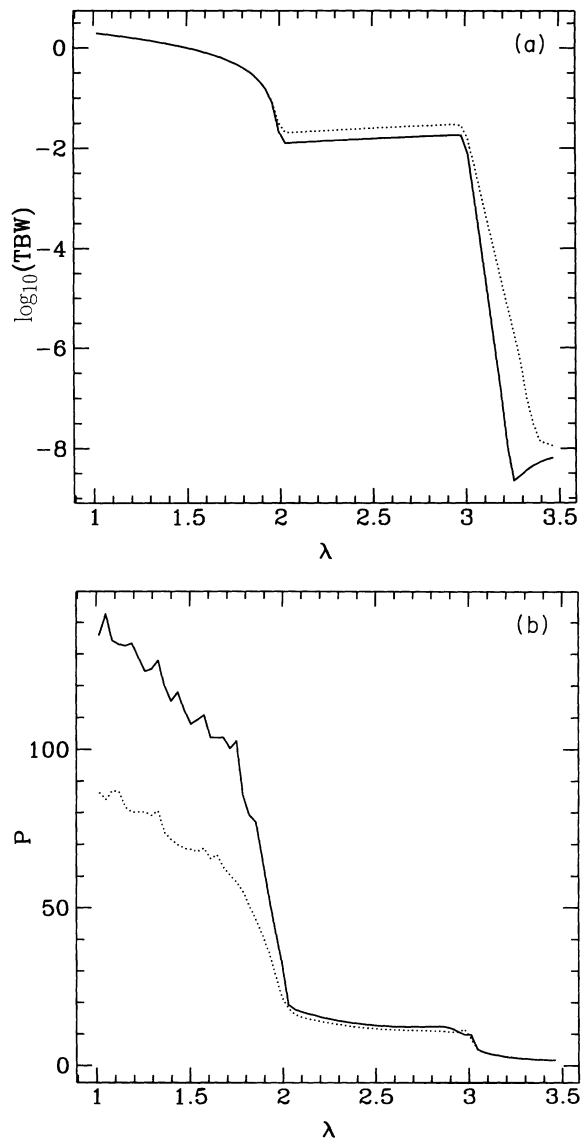


FIG. 2. (a)-(b) show TBW and  $P$  for  $g = 0.5$ ,  $\sigma = 233/377$ . Dotted lines are the corresponding curves for  $\sigma = 144/233$ . The two transitions,  $E$ - $C$  and  $C$ - $L$  are clearly seen in the variation of both TBW and  $P$ , with respect to  $\lambda$ . In the  $C$  phase,  $P$  is almost independent of the size of the chain.

$C$  and  $C-L$  transitions are, respectively, determined by the strength of the exchange interactions along the hard and easy axes and the width of the  $C$  phase is solely determined by the spin space anisotropy. In the Ising limit, one sees a single transition from the  $C$  to  $L$  phase and the model does not support any  $E$  phase as was reported earlier.<sup>14</sup>

It is interesting that the  $E-C$  and  $C-L$  transitions are, respectively, signaled by the maxima and minima in the ratio  $R$  which is defined as the ratio of the gap to the width of the lowest band. (See Fig. 3.) In previous studies of the Harper equation,<sup>15</sup>  $R$  was found to converge to a universal value for the golden mean case (exhibiting period-three behavior as successive rational approximants are used) at the onset of the  $E-L$  transition. In the

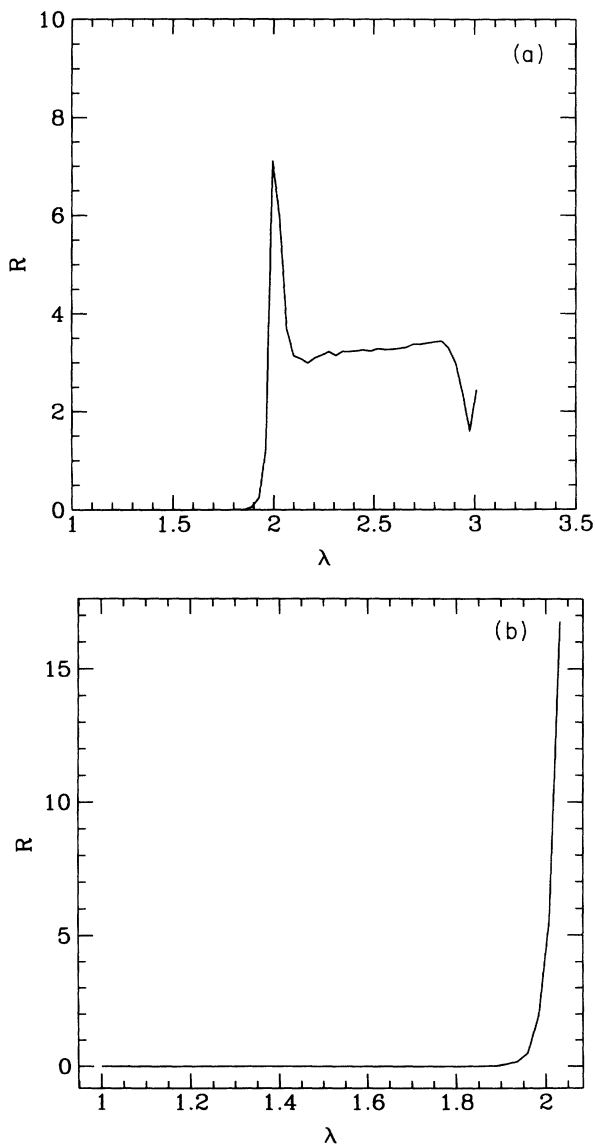


FIG. 3. (a) and (b), respectively, show the variation in  $R$  with  $\lambda$  for  $g = 0.5$  and  $g = 0$ .  $E-C$  and  $C-L$  transitions in the anisotropic case are, respectively, characterized by a maxima and a minima in  $R$ . In the isotropic case,  $R$  is found to diverge beyond the transition point,  $\sigma = 233/377$ .

anisotropic case, the minimum value of  $R$  at the onset of the  $C-L$  transition is always found to converge to a universal ratio, which exhibits period three as a sequence of Fibonacci periods are used. On the contrary, the maxima in  $R$  signaling the transition from the extended to critical phase shows no such convergence. However, these  $R$  values obtained in the anisotropic case are  $g$  dependent and are different from those of the Harper model. For example, instead of 1.37 and 7.81, the  $R_1 - R_2$  values for the  $g = 1$  case are found to be 1.5 and 6.88 while the corresponding values for the Ising model are 0.62 and 2.4.

Figure 4 summarizes the spectral phase diagram in the  $g-\lambda$  plane for a fixed value of  $J_x$ . We see that the self-dual point for the isotropic model or Harper equation is in fact a tricritical point corresponding to the coexistence of  $E$ ,  $L$ , and  $C$  phases. For any finite value of  $g$ , the  $C$  phase exists in a finite window sandwiched between the  $E$  and  $L$  phases. It should be pointed out that the spectral phase diagram is in fact determined by the absolute values of the exchange couplings  $J_x$  and  $J_y$ . Hence the spectral phase diagram for both the ferromagnetic and antiferromagnetic exchange interactions are identical.

#### IV. SPECTRAL AND MAGNETIC INTERPLAY

The eigenvalues and eigenfunctions obtained by exact numerical diagonalization of the fermionic quadratic form can be used to compute the long-range spin-spin correlations along the easy axis  $C_n^e(N) = \langle \sigma_n^e \sigma_{n+N}^e \rangle$  as well as along the transverse direction  $C_n^z(N) = \langle \sigma_n^z \sigma_{n+N}^z \rangle$ .<sup>10</sup> Here  $N$  is the maximum possible distance between two lattice sites on the periodic chain.

Our numerical results indicate that the onset of magnetic transition coincides with the onset of the spectral

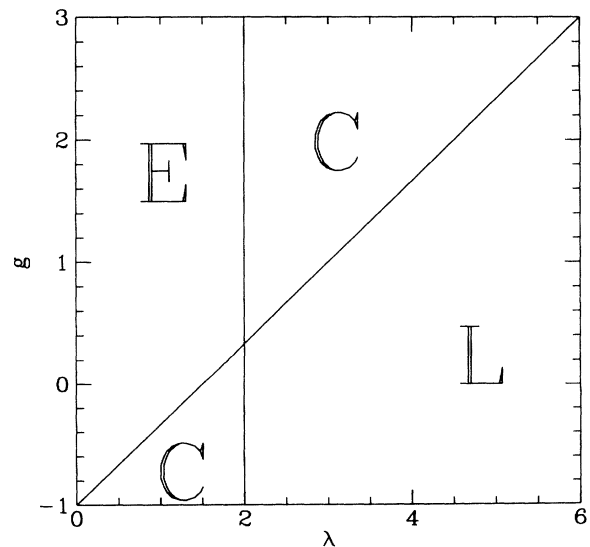


FIG. 4. The spectral phase diagram in the  $g$  and  $\lambda$  plane for  $J_x = 1$ . The hatched region marked as  $C$  shows the critical phase. The extended and localized phases are, respectively, labeled as  $E$  and  $L$ .  $g = 0$  is clearly a special point where the  $E$ ,  $C$ , and  $L$  phases coexist.

transition from the  $C$  to  $L$  phases as shown in Fig. 1 in Ref. 9. Both the  $E$  and  $C$  phases support long-range correlations in the  $XY$  plane. Furthermore, the spectral transition seems to have no bearing on the magnetic transition and the long-range two-point spin-spin correlation function varies smoothly across the spectral transition. This is somewhat surprising in view of the fact that the wave functions are smooth Bloch-type in  $E$  phase and fractal in  $C$  phase. We speculate that the averaging associated with the definition of the long-range correlation functions wipes out any possible singularities that the  $E$ - $C$  transition could possibly have on the magnetic correlations.

For periodic systems,  $C_n(N)$  are  $n$  independent and in the large  $N$  limit decay to zero as  $C_n(N) \sim (\lambda - \lambda_c)^{1/4}$

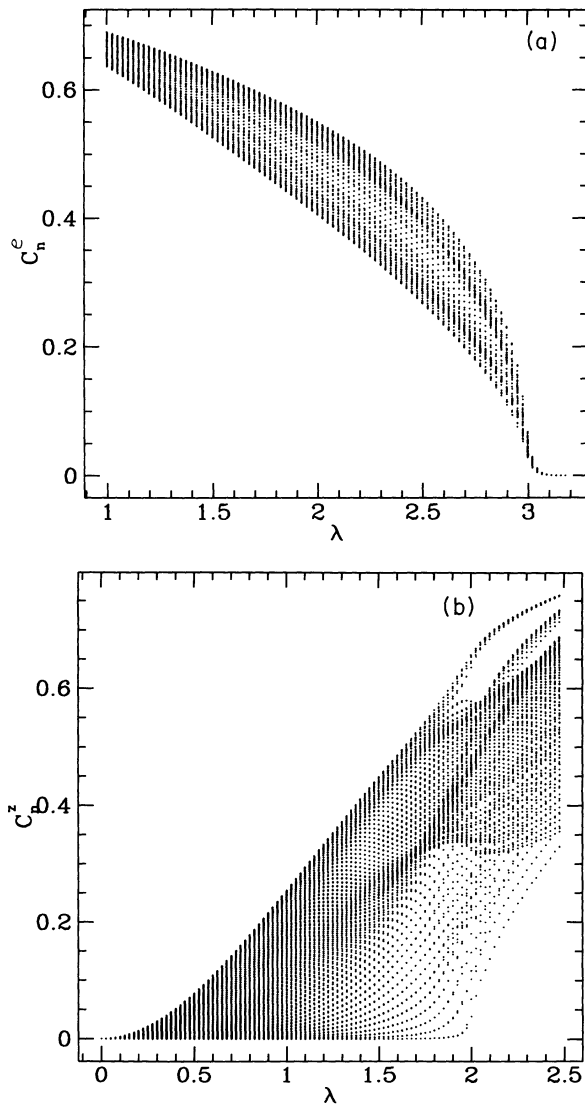


FIG. 5. (a) Long-range correlation function along the easy axis,  $C_n^e(N)$  vs  $\lambda$  for  $g = 0.5$ ,  $\sigma = 144/233$  with different points along the  $y$  axis showing the  $n$  dependence of spin correlations between site  $n$  and the site  $n + N$  ( $N = 117$ ) along the periodic chain. (b)  $C_n^z(N)$  vs  $\lambda$  for  $g = 0$ . Note that the correlations along the easy axis are zero in this case.

near the critical point  $\lambda_c$ . For the quasiperiodic case,  $C_n(N)$  are site ( $n$ ) dependent. However, the average value of  $C_n(N)$ , averaged over all sites, behave like the periodic system (Fig. 5). Therefore, the quasiperiodic anisotropic models belong to the universality class of the periodic Ising model. The new feature associated with the long-range correlations in the quasiperiodic model is the existence of modulations in  $C_n(N)$  along the chain. For the isotropic case, due to the lack of preferred direction in the plane, in-plane magnetization is zero. The spectral transition from the  $E$  to  $L$  phase corresponds to a magnetic transition where all the spins have *finite* correlations in the  $z$  direction. [See Fig. 5(b).] The  $E$  phase is always massless (i.e., has a zero-frequency mode) and the  $E$ - $L$  transition corresponds to the disappearance of the zero-frequency mode corresponding to the breaking of the translational invariance. A rather complex spatial

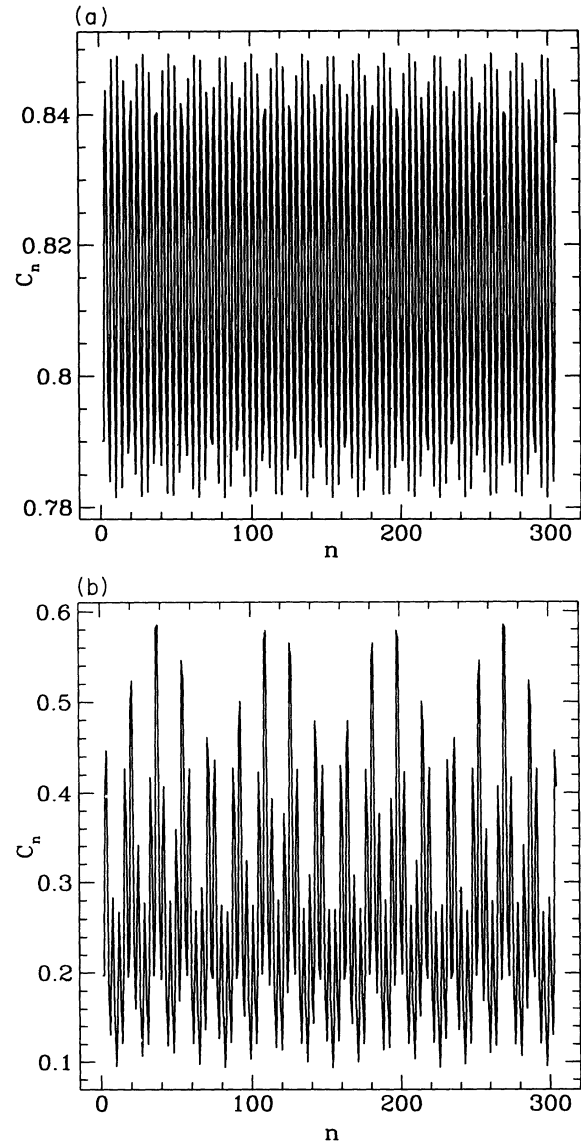


FIG. 6. The variation in long-range correlations at different sites for  $g = 1$  and  $\lambda = 1$  (a) and  $\lambda = 3.8$  (b), respectively.  $\sigma = 377/610$ .

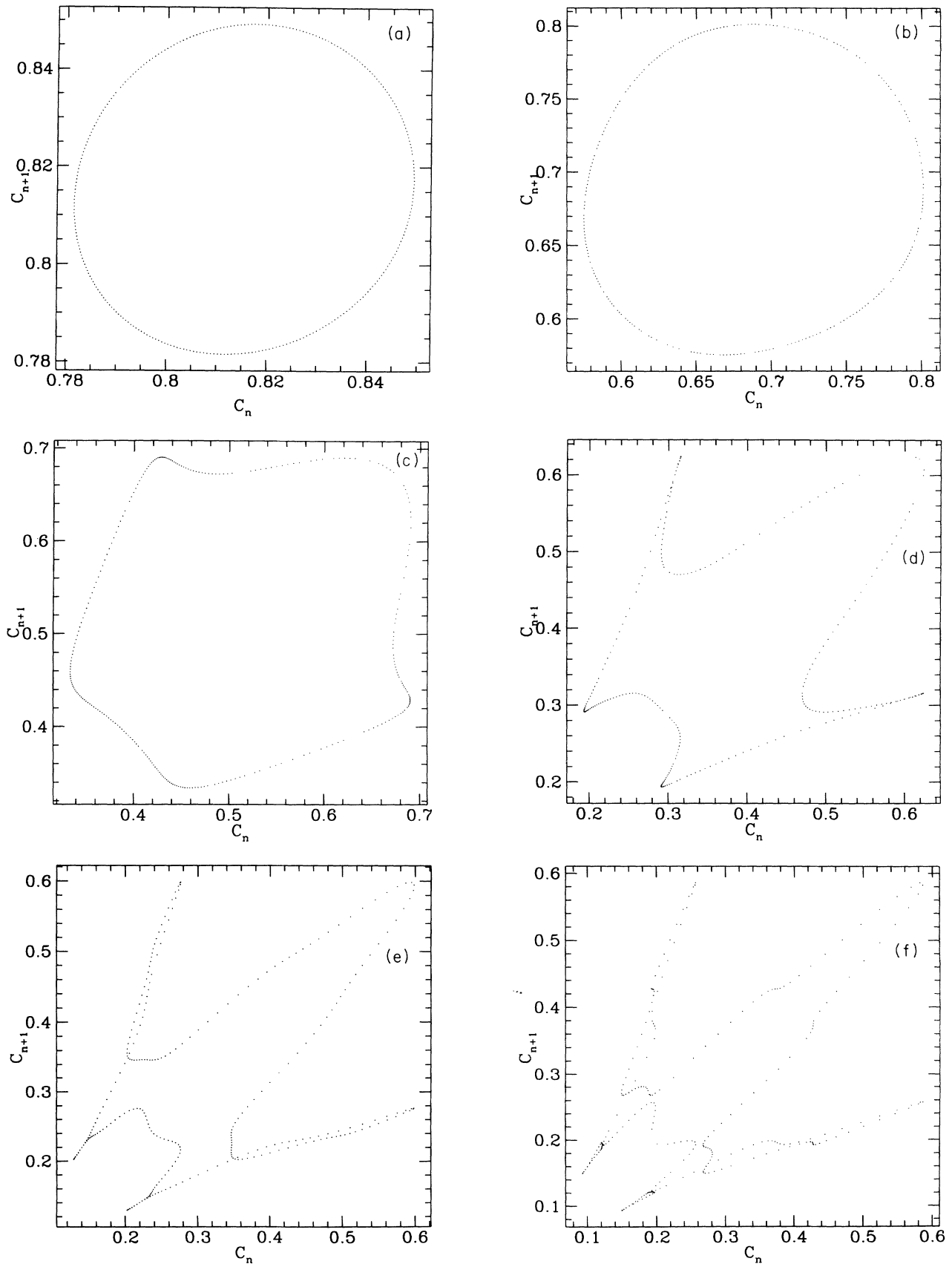


FIG. 7. (a)–(f) Return map [plot of  $C_n^e(N)$  vs  $C_{n+1}^e(N)$ ] for the spin-spin correlation function for  $\lambda$  equals 1, 2, 3, 3.5, 3.7, 3.8, respectively.  $g = 1$  and  $\sigma = 377/610$ .

dynamics is clearly visible near the onset to transition and requires further investigation.

We further investigate the site dependence of  $C_n(N)$  for the anisotropic models in Figs. 6 and 7. These figures describe the complexity and richness underlying the spatial dynamics which is a consequence of quasiperiodicity. Near the onset of magnetic transition,  $C_n(N)$  exhibits behavior characteristic of a fractal set (Fig. 6). Further insight in the spatial dynamics of the anisotropic quasiperiodic chain is obtained by studying the return map of  $C_n(N)$  (Fig. 7). Our numerical results show that mapping of  $C_n(N)$  to  $C_{n+1}(N)$  defines a one-dimensional torus which is topologically equivalent to a circle. We will refer to this torus as a magnetic torus. It is interesting to note that this magnetic torus is a smooth curve in the  $E$  phase. However, in the  $C$  phase, it begins to get distorted by becoming more wrinkled as  $\lambda$  increases and disappears in the  $L$  phase suggesting a new catastrophic mechanism for the disappearance of a torus. Therefore, the magnetic transition in the quasiperiodic model can be described by this magnetic torus.

## V. GLOBAL SCALING IN THE CRITICAL PHASE

In the  $C$  phase the cantor spectrum of the fermions is a multifractal with a distribution of continuously varying exponents  $\alpha$  varying in a range  $(\alpha_{\min}, \alpha_{\max})$  with each  $\alpha$  value associated with its own fractal dimension  $f(\alpha)$ . Hence this multifractal is fully characterized by the  $f(\alpha)$  curve.<sup>16</sup> The exponent  $\alpha$  is related to the scaling of integrated density of states  $D(E)$  as follows. The spectrum has a scaling index  $\alpha$  at energy  $E$  if  $D(E)$  behaves as<sup>17</sup>

$$D(E + \Delta E) - D(E) \approx (\Delta E)^\alpha, \quad \Delta E \rightarrow 0, \quad (7)$$

where  $E$  and  $E + \Delta E$  are both in the spectrum. This scaling index  $\alpha$  is different in different parts of the spectrum. Therefore, all the information about the global scaling properties of the system are contained in the  $f(\alpha)$  curve. The Hausdorff dimension  $D_H$  of the energy spectrum is the maximum value of  $f(\alpha)$ . The  $f(\alpha)$  curve and the denumerable set of dimensions can be determined using the thermodynamical formalism.<sup>16</sup> For  $\sigma = F_{l-1}/F_l$ , we define the partition function of the set of  $F_l$  bands as

$$\Gamma_l(q, \tau) = \sum (F_l)^q / (\omega_i)^\tau, \quad (8)$$

where  $\omega_i$  is the width of the  $i$  band and  $F_l^{-1}$  is its measure. The condition  $\Gamma(q, \tau) = \lim_{l \rightarrow \infty} \Gamma_l = 1$  gives  $\tau(q)$ . The generalized Renyi dimensions<sup>18</sup>

$$D_q = \tau / (q - 1) \quad (9)$$

characterize the fractal set in terms of  $\infty$  of dimensions with  $D_0$  being the Hausdorff dimension. This spectrum of dimensions is linked to the spectrum scaling indices  $f(\alpha)$  by the Legendre transformation,

$$\alpha = \frac{d\tau}{dq}, \quad (10)$$

$$f(\alpha) = q\alpha - \tau. \quad (11)$$

In the  $E$  phase the scaling is trivial with a single index  $\alpha = 1$  almost everywhere in the spectrum except at zero measure band edges with Van Hove singularities where  $\alpha = 0.5$ .<sup>17</sup> However, in the  $L$  phase, there is no scaling. In the  $C$  phase,  $f(\alpha)$  is a continuous curve. Therefore, the  $f(\alpha)$  computation serves as a useful diagnostic to confirm the spectral phase diagram shown above. Since the multifractal set is a fat set in parameter space, the  $f(\alpha)$  curve also summarizes in a rather useful way how the scaling properties of the fractal set vary as  $g$  and  $\lambda$  are varied.

Figure 8 shows how the  $f(\alpha)$  curve of the isotropic model is modified in the presence of  $g$  and also how it varies at different points in the  $C$  phase. Our nu-

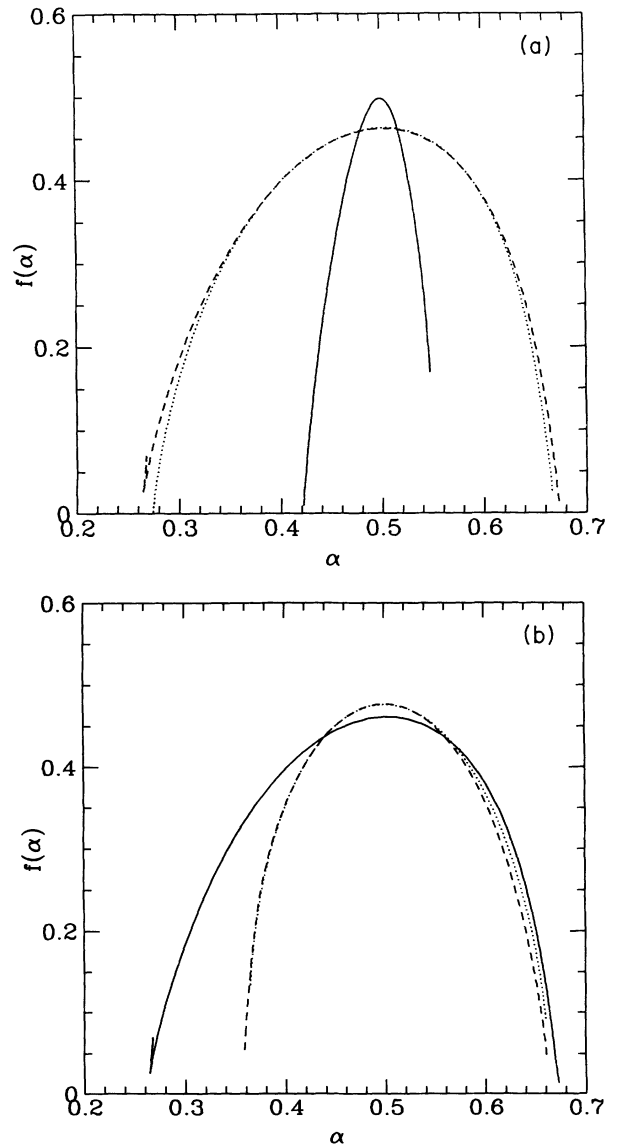


FIG. 8. (a) The  $f(\alpha)$  curve for fixed  $\lambda = 2$  and  $g = 0$  (solid line),  $g = 1$  (dashed line) and  $g = 0.5$  (dotted line). (b)  $f(\alpha)$  for fixed  $g = 1$  and  $\lambda = 2$  (solid line),  $\lambda = 3$  (dashed line), and  $\lambda = 3.5$  (dotted lines). Curves are calculated from  $\Gamma_{11}/\Gamma_{14} = 1$ .

merical results show that for all values of  $g$  and  $\lambda$  the  $f(\alpha)$  shows a peak at  $\alpha = 0.5$ . However, the range of  $\alpha$  values ( $\alpha_{\min}, \alpha_{\max}$ ) show considerable differences in the isotropic and nonisotropic cases. For finite fixed  $g$ , as  $\lambda$  is varied, the  $f(\alpha)$  curve shows significant variation in the vicinity of the E-L transition and cease to exist beyond the C-L transition.

$\alpha_{\min}$  and  $\alpha_{\max}$ , respectively, correspond to the scaling of the most dense and most ramified regions of the spectrum, i.e.,  $D(E)$  varies as  $\Delta E^{\alpha_{\min}}$  as  $E \rightarrow 0$  and  $\Delta E^{\alpha_{\max}}$  as  $E \rightarrow E_{\max}$ .  $\alpha_{\min}$  determines the specific heat and zero-field susceptibility exponents at low temperatures. Hence for Ising-like QP spin chains the scaling exponents vary continuously in the C phase.

## VI. HIGHER HARMONIC MODEL

In a recent study,<sup>19</sup> the extended Harper model, where the sinusoidal variation of the potential or magnetic field contains two harmonics, was studied:

$$h_n = \frac{\lambda}{\sqrt{(1 + \alpha^2)}} [\cos(2\pi\sigma n) + \alpha \cos(4\pi\sigma n)]. \quad (12)$$

Unlike the single harmonic case, the model exhibits a mixed spectrum where different quantum states undergo E-L transition at different values of the parameter. Furthermore, each quantum state exhibits a cascade of E-L phases where the boundary between the existence and nonexistence of the two phases was a fractal in the  $\lambda, \alpha$  plane. Therefore, the isotropic XY model has a devil-fork phase diagram in the two-parameter space. Underlying these cascades of transitions are cascades of band crossings between the two lowest-energy bands of the XY model. The band crossings which are absent in the single harmonic XY model have a very special significance in the two-harmonic model. They were sandwiched between two successive metal-insulator transitions of the incommensurate model. Furthermore, the band crossings were found to exhibit *additive rules*: the number of crossings in the  $n$ th order Farey tree is equal to the sum of the crossings in the two previous Farey daughters. These additive rules in the incommensurate limit imply the fractal boundary which is believed to be a cantor set of measure zero.

In view of the exotic behavior of the isotropic XY model, we investigate the effect of spin space anisotropy on the fractal boundary and the band crossings. Our studies show that some of the band crossings disappear in the presence of infinitesimal anisotropy. (See Fig. 2 in Ref. 10.) Extensive numerical studies showed that the anisotropy destroys the additive rules for the band crossings and hence the fractal boundary. However, the system could have a finite number of E-L transitions corresponding to a finite number of reentrances to the localized phase. We speculate that the existence of long-range spin-spin correlations destroys the fractal phase boundary of the isotropic model.

## VII. CONCLUSIONS

The spectral phase diagram of the anisotropic quantum XY spin chain consists of a fat critical phase in addition to extended and localized phases. In the isotropic limit, the critical phase degenerates to a tricritical point where the E, C, and L phases coexist. In other words, the anisotropy fattens the critical point of the isotropic model stabilizing it in a finite measure window in parameter space. The transition to exponentially localized states is accompanied by a magnetic transition to LRO. Unlike the periodic case, the onset to LRO is determined by the strength of the exchange interaction along the easy axis only. The onset of E-C spectral transition determined by the exchange interaction along the hard axis has no effect on the magnetic transition.

Our studies provide a new paradigm in the theory of metal-insulator transition in one dimension where the metallic phase with smooth Bloch states remain singular continuous for a while before becoming discontinuous. The existence of a critical phase with power-law localization has rather interesting consequences on the thermodynamical properties of the system. Our studies show that the low-temperature specific heat exponent varies continuously in the C phase.

The presence of LR interactions in the model are known to reduce the critical dimensionality of various phase transitions.<sup>20</sup> Our spin Hamiltonian involves only NN interactions. We speculate that the dynamically generated long-range magnetic correlations lower the critical dimensionality of power-law localization resulting in the existence of such a phase in one-dimensional models. For our spin model, the QP disorder is trying to localize the system whereas the long-range correlations try to resist localization. The intermediate C phase is like a compromise phase where the system is neither extended nor exponentially localized. This picture is consistent with the fact that the onset to localization is accompanied by the vanishing of LRO. This second-order phase transition accompanied by the appearance of a zero-frequency mode is believed to play an important role in the three-phase spectral diagram. Preliminary studies of an anisotropic spin chain in the presence of an analytic pseudorandom magnetic field<sup>21</sup> indicate the existence of a fat C phase in the neighborhood of a magnetic transition (signaled by a zero mode), sandwiched between localized phases. In summary, the isotropic model remains extended until the QP disorder is strong enough (compared to the exchange interaction) to localize the system resulting in a two-phase diagram. However, the anisotropic model provides an additional competition between the long-range correlations and QP disorder resulting in a three-phase diagram.

The spectral phase diagram with E, C, and L phases also have interesting and perhaps experimentally realizable consequences on the magnetic properties as well. The return map of the site dependent long-range correlations is an attractor which happens to be a one-dimensional torus. This magnetic torus is smooth in the E phase and gets much more wrinkled in the C phase and disappears beyond the onset of the C-L transition.

This scenario for the disappearance of the magnetic torus, although reminiscent of the breakdown of KAM tori in Hamiltonian maps, is characteristically different from it. Unlike the KAM torus, which degenerates to a cantorus beyond the onset of transition, the magnetic torus disappears at the onset of transition. This behavior is suggestive of a new type of catastrophic behavior for the disappearance of a torus in nonlinear systems and requires further investigation.

In view of the similarity between the TBM model and area preserving map, it is interesting to conjecture what bearing these results may have on the Hamiltonian maps. Our new scenario for metal-insulator transition suggests a new paradigm for the breaking of the KAM tori where the torus will remain critical in a finite regime of the parameter space before breaking. However, the existence of such a scenario in area preserving maps has not been known.

The emergence of a new scenario for breakdown of analyticity in one-dimensional QP systems associated with the existence of fat critical set is an important result.

This paper describes a class of spin models exhibiting this behavior. Our conjecture linking the fattening of the critical point to the magnetic long-range correlations may be one of many possible mechanisms for the stabilization of the  $C$  phase. General conditions and criteria for this novel behavior remain an open question. Since the  $C$  phase exists in a finite measure interval, the physical realization of fractality and its consequences in experiments involving magnetic superlattices may be possible.

#### ACKNOWLEDGMENTS

I would like to thank Bala Sundaram for various fruitful discussions and suggestions during the course of this work and for critically reading this manuscript. This research was supported by a grant from National Science Foundation DMR 093296. I would like to acknowledge the hospitality of Magnetic Materials group at National Institute of Standard and Technology where part of this work was done.

\* Electronic mail address: isatija@sitar.gmu.edu.

- <sup>1</sup> P. G. Harper, Proc. Phys. Soc. London, Sect. A **68**, 874 (1955).
- <sup>2</sup> For review, see J. B. Sokoloff, Phys. Rep. **126**, 189 (1985).
- <sup>3</sup> D. R. Hofstadter, Phys. Rev. B **14**, 2239 (1976).
- <sup>4</sup> D. J. Thouless, in *Quantum Hall Effect*, edited by R. Prange and S. M. Girvin (Springer-Verlag, Berlin, 1990).
- <sup>5</sup> I. Affeck and J. B. Maston, Phys. Rev. B **37**, 3774 (1988).
- <sup>6</sup> R. R. Gerhart, D. Weiss, and K. V. Klitzing, Phys. Rev. Lett. **62**, 1173 (1989).
- <sup>7</sup> See V. I. Arnold and A. Avez, *Ergodic Problems of Classical Mechanics* (Benjamin, New York, 1968).
- <sup>8</sup> R. S. Mackay, Ph.D. thesis, Princeton University, 1982.
- <sup>9</sup> I. I. Satija, Phys. Rev. B **48**, 3511 (1993).
- <sup>10</sup> E. Lieb, T. Schultz, and D. Mattis, Ann. Phys. (N.Y.), **16**, 407 (1961); M. Doria and I. Satija, Phys. Rev. Lett. **60**, 444 (1988).
- <sup>11</sup> It should be noted that the quantum Ising model in a transverse field can be mapped to a two-dimensional classical Ising model with QP exchange interaction along one of the directions. Therefore, our studies may have some experimental relevance in modulated two-dimensional superlattices.
- <sup>12</sup> E. Fradkin and L. Susskind, Phys. Rev. D **17**, 2637 (1978).
- <sup>13</sup> S. Aubry and C. Andre, *Proceedings of the Israel Physical Society* (Hilger, Bristol, 1979), Vol. 3, p. 133.
- <sup>14</sup> I. I. Satija and M. Doria, Phys. Rev. B **39**, 9757 (1989); **41**, 7235 (1990).
- <sup>15</sup> H. J. Schellnhuber and H. Urbschat, Phys. Rev. Lett. **54**, 588 (1985); Phys. Status Solidi B **140**, 509 (1987).
- <sup>16</sup> T. C. Halsey, M. H. Jensen, L. P. Kadanoff, I. Procaccio, and B. I. Shraiman, Phys. Rev. A **33**, 1141 (1986).
- <sup>17</sup> C. Tang and M. Khomoto, Phys. Rev. B **34**, 2041 (1986).
- <sup>18</sup> A. Renyi, *Problem Theory* (North-Holland, Amsterdam, 1970).
- <sup>19</sup> R. C. Black and I. I. Satija, Phys. Lett. **157**, 246 (1991); R. C. Black and I. I. Satija Phys. Rev. Lett. **65**, 1 (1990); Phys. Rev. B **44**, 4089 (1991).
- <sup>20</sup> See, for example, A. Singh and B. Sundaram, Phys. Lett. A **145**, 232 (1990); also I. Satija and B. Sundaram (unpublished).
- <sup>21</sup> I. I. Satija (unpublished).